Research Article

Osteopontin Promotes Vascular Endothelial Growth Factor–Dependent Breast Tumor Growth and Angiogenesis via Autocrine and Paracrine Mechanisms

Goutam Chakraborty, Shalini Jain, and Gopal C. Kundu

National Center for Cell Science, Pune, India

Abstract

Angiogenesis is the hallmark of cancer, and development of aggressiveness of primary tumor depends on *de novo* angiogenesis. Here, using multiple *in vitro* and *in vivo* models, we report that osteopontin (OPN) triggers vascular endothelial growth factor (VEGF)–dependent tumor progression and angiogenesis by activating breast tumor kinase (Brk)/nuclear factor–inducing kinase/nuclear factor-κB (NF-κB)/activating transcription factor-4 (ATF-4) signaling cascades through autocrine and paracrine mechanisms in breast cancer system. Our results revealed that both exogenous and tumor-derived OPN play significant roles in VEGF-dependent tumor angiogenesis. Clinical specimen analysis showed that OPN and VEGF expressions correlate with levels of neuropilin-1, Brk, NF-κB, and ATF-4 in different grades of breast cancer. Consequently, OPN plays essential role in two key aspects of tumor progression: VEGF expression by tumor cells and VEGF-stimulated neovascularization. Thus, targeting OPN and its regulated signaling network could be a novel strategy to block tumor angiogenesis and may develop an effective therapeutic approach for the management of breast cancer. [Cancer Res 2008;68(1):152–61]

Introduction

Angiogenesis, the formation of new blood vessels from the existing one is a key step for tumor growth, survival, progression, and metastasis (1). A large number of proangiogenic factors and their cognate receptors have been identified (2–4). To date, the best characterized proangiogenic cytokine to turn on the "angiogenic switch" is vascular endothelial growth factor (VEGF; ref. 5). For over a decade, the role of VEGF in regulation of tumor angiogenesis has been under intense investigation (6). Previous results indicated that VEGF signaling represents a critical rate-limiting step in angiogenesis (7). Alternative exon splicing results in four isoforms of VEGF ($VEGF_{121}$, $VEGF_{165}$, $VEGF_{189}$, and $VEGF_{206}$), and among them, $VEGF_{165}$ is the predominant one that plays a major role in tumor angiogenesis (7, 8). Recent data show that the functions of VEGF may not be limited to endothelial cells but also play important roles in survival, proliferation, and migration in tumor cells (9, 10).

Osteopontin (OPN), a secreted noncollagenous, sialic acid–rich, chemokine-like protein and also a member of small integrin-binding ligand N-linked glycoprotein family plays important role in determining the oncogenic potential of various cancers (11, 12). OPN exerts its prometastatic effects by regulating various cell signaling events through interaction with integrins and CD44 receptors that ultimately lead to tumor progression (13). Recent evidences indicated that OPN regulates tumor growth through induction of cyclooxygenase-2 and urokinase-type plasminogen activator expressions and activation of matrix metalloproteinases in various cancer cells (14–17). The role of OPN in various pathophysiologic conditions, particularly in cancer, suggested that the variation in glycosylation, phosphorylation, and sulfation generates the different functional forms that might alter its normal physiologic functions (12, 18). Previous studies have shown that tumor-derived OPN is soluble, and it exhibits close similarity with human milk OPN (19, 20). Earlier reports also suggested that OPN produced either from tumor or stromal cells has been shown to enhance the metastatic ability (21).

Breast tumor kinase (Brk/PTK6/Sik) is a nonreceptor tyrosine kinase and expressed in metastatic breast tumors but not in normal mammary tissue or benign lesions (22). It has been postulated that Brk promotes cell migration, and silencing of Brk resulted in inhibition of migration and proliferation in various cancer cells, including MDA-MB-231 (23, 24). Recent data revealed that activating transcription factor-4 (ATF-4/cAMP-responsive element binding protein-2) regulates VEGF expression (25, 26). Neuropilin-1 (NRP-1) was initially characterized to mediate the chemorepulsive activity of collapsin/semaphorins in neuronal cells (27, 28). NRP-1 is also expressed in endothelial cells and in various tumors, and it functions as isoform-specific receptor for $VEGF_{165}$ and plays an important role in tumor progression (29–32). Previous studies have shown that blocking or silencing of NRP-1 resulted in significant reduction of tumor progression (10). However, the role of Brk in regulation of ATF-4–dependent VEGF expression and interaction of VEGF with NRP-1 in response to OPN and how all of these ultimately control breast tumor angiogenesis is not well defined.

In this study, we provide both *in vitro* and *in vivo* experimental evidences that show the molecular mechanism by which OPN regulates Brk/nuclear factor-κB (NF-κB)/ATF-4 signaling cascades that ultimately augment the VEGF expression and tumor angiogenesis through autocrine and paracrine mechanisms. We have further substantiated the crucial roles of tumor-derived, endogenous OPN in tumor angiogenesis using short interfering RNA (siRNA) based approach in *in vitro* and *in vivo* models. Moreover, our clinical data revealed that the enhanced expressions of OPN and VEGF correlate with NRP-1, Brk, NF-κB and ATF-4 levels in breast carcinoma of higher grades. These data provide new insights into the mechanism underlying the regulation of VEGF expression by OPN in breast tumor angiogenesis and understanding these mechanisms may form the basis of new therapeutic regimens for the management of breast cancer.

Note: Supplementary data for this article are available at Cancer Research Online (http://cancerres.aacrjournals.org/).

Requests for reprints: Gopal C. Kundu, National Center for Cell Science, Pune 411 007, India. Phone: 91-20-25708103; Fax: 91-20-25692259; E-mail: kundu@nccs.res.in.

doi:10.1158/0008-5472.CAN-07-2126

Materials and Methods

Cell culture and transfection. Human breast adenocarcinoma (MDA-MB-231) cell line was obtained from American Type Culture Collection. Human umbilical vein endothelial cell line EA.hy-926 was a generous gift from Dr. Christopher Newton. The super repressor form of IκBα in pCMV4 (Dr. Dean Ballard, Vanderbilt University School of Medicine), wild-type (wt) and kinase negative (mut) nuclear factor–inducing kinase (NIK; K249A/K430A) in pcDNA3 vector (Prof. David Wallach, Weizmann Institute of Science), VEGF-Luc construct (Dr. Debabrata Mukhopadhyay, Mayo Clinic College of Medicine), VEGF-GFP cDNA construct (Dr. Rakesh K. Jain, Massachusetts General Hospital), wt (pEF/mATF-4) and dominant-negative (dn; pEF/mATF-4M) ATF-4 (Dr. Javed Alam, Yale University School of Medicine), wt and kinase mutant (KM) Brk in pRC CMV vector (Prof. Mark Crompton, Royal Holloway University of London), and human OPN cDNA in pcDNA 3.1 (Dr. Ann Chambers, University of Western Ontario) were transfected in MDA-MB-231 cells using Lipofectamine 2000.

siRNA. Cells were transfected with OPN siRNA (OPNi) or NRP-1 siRNA (NRP-1i; Dharmacon) using liposome according to manufacturer's instructions. The sequence targeted for OPN is 5′ GUU UCA CAG CCA CAA GGA CdTdT/dTdT CAA AGU GUC GGU GUU CCU G 5′ and its nonsilencing control is 5′ CAG UAC AAC GCA UCU GGC AdTdT/dTdT GUC AUG UUG CGU AGA CCG U 5′. The NRP-1 siRNA sequence is 5′ GAG AGG UCC UGA AUG UUC CdTdT/dTdT CUC UCC AGG ACU UAC AAG G 5′ and its nonsilencing control is 5′ AGA GAU GUA GUC GCU CGC UdTdT/dTdT UCU CUA CAU CAG CGA GCG A 5′. The Brk siRNA sequence is 5′AAG GUG GCC AUU AAG GUG AdTdT/dTdT UUC CAC CGG UAA UUC CAC U 5′ and its nonsilencing control is 5′CAC ACU AGG UUG CCA CAG GdTdT/dTdT GUG UGA UCC AAC GGU GUC C 5′.

Purification of human OPN. The human OPN was purified from human breast milk as described previously with minor modifications and used throughout this study (15).

Coculture assay. The tumor-endothelial cell interaction was studied by coculture experiments using MDA-MB-231 and EA.hy-926 cells. EA.hy-926 cells were transfected with NRP-1i and cocultured with nontransfected or OPNi or NRP-1i transfected MDA-MB-231 cells. In separate experiments, cocultured cells were either treated with OPN alone or along with anti-VEGF antibody. The level of pKDR in cell lysates was detected by immunoprecipitation followed by Western blot.

Immunoprecipitation and Western blot. The immunoprecipitation and immunoblot experiments were performed using their specific antibodies as described (14).

RNA extraction and reverse transcription–PCR. The RNA was isolated from MDA-MB-231 cells and used for reverse transcription–PCR (RT-PCR). The VEGF primers were used: sense, 5′-CCC TCC GAA ACC ATG AAC TTT-3′ and antisense, 5′-AGA GAT CTG GTT CCC GAA AC-3′. The amplified cDNA fragments were resolved by agarose gel electrophoresis.

Reporter gene expression. MDA-MB-231 cells were transfected with VEGF-luciferase reporter construct, either alone or along with OPN cDNA or OPNi. Cell lysates were analyzed by Western blot using antiluciferase antibody. The VEGF promoter activity was measured either by transfecting MDA-MB-231 cells with VEGF-GFP or cotransfected with wt and KM Brk or wt and dn ATF-4 or IκBα super repressor (sup. rep.) or Brk siRNA and then treated with OPN. The GFP expression was measured by using fluorescence microscopy (Nikon) and quantified by Image Pro Plus 6.0 Software (Nikon) and represented in the form of bar graph.

Brk kinase assay. Brk kinase assay was performed as described earlier (22).

EMSA. MDA-MB-231 cells were either transfected with wt and KM Brk or wt and mut NIK, IκBα sup. rep. or wt and dn ATF-4 and then treated with 0.5 μmol/L OPN. Nuclear extracts were used for NF-κB and ATF-4–DNA binding.

Immunofluorescence. To examine whether OPN regulates ATF-4 expression and nuclear translocation, MDA-MB-231 cells were treated with 0.5 μmol/L OPN, and immunofluorescence was performed using anti–ATF-4 antibody.

Wound migration. The wound assay was performed using MDA-MB-231 and endothelial (EA.hy-926) cells with typical cobblestone morphology as described (14).

Cell comigration assay. The endothelial-breast tumor cell interaction was shown by comigration assays. MDA-MB-231 cells were treated with either OPN alone or along with anti-VEGF or anti–NRP-1 blocking antibody and used in lower chamber. EA.hy-926 cells were seeded on the upper chamber. In separate experiments, MDA-MD-231 cells were transfected with OPNi or NRP-1i and used for comigration assay. The migrated cells were stained with Giemsa and were counted in three high-power fields under an inverted microscope.

***In vivo* Matrigel-based angiogenesis assay.** The *in vivo* Matrigel angiogenesis assay was preformed as described (33). Briefly, Matrigel (0.5 mL) was injected s.c. in the ventral groin region of female athymic NMRI (nu/nu) mice. In separate experiments, the conditioned medium (CM) of untreated or OPN-treated MDA-MB-231 cells were mixed with Matrigel and injected to the mice. In other experiments, OPN-treated CM was mixed with anti-VEGF blocking antibody (400 μg/kg of body weight per mice) and Matrigel or CM collected from OPNi-transfected cells were mixed with Matrigel and then injected to the mice. After 3 weeks, Matrigel plugs were excised and processed for histopathology and immunohistochemistry. The paraffin sections were immunostained with antihuman vWF and anti–phosphorylated KDR antibodies.

***In vivo* tumorigenicity, histopathology, and immunohistochemistry.** The tumorigenicity and immunohistochemistry experiments were performed as described earlier (34, 35). Briefly, MDA-MB-231 (5×10^5) cells were injected orthotopically in the mammary fat pad of female athymic nude mice. OPN (0.5 μmol/L) or anti-VEGF (400 μg/kg of body weight per mice) blocking antibody was injected to the site of tumor twice a week up to 6 weeks. In other experiments, OPN cDNA transfected cells alone or along with anti-VEGF antibody were injected into the nude mice. In separate experiments, OPNi or NRP-1i (250 μg/kg of body weight per mice) mixed with transfection reagent were given to the site of tumor twice a week until termination of the experiments. Mice were sacrificed and photographed, the tumors were dissected out and weighed, and tumor tissues were used for histopathologic and immumohistochemical studies with their specific antibodies. Tumor samples were lysed in lysis buffer. Mice blood was collected from retro-orbital plexus, and serum was isolated. The levels of OPN, VEGF, and CA 15-3 were detected by Western blot using their specific antibodies. The OPN-induced VEGF–NRP-1 interaction in tumor samples was analyzed by immunoprecipitating tumor lysates with anti-VEGF antibody and immunoblotted with anti–NRP-1 antibody. The nuclear extracts of tumor tissues were prepared as described earlier and used for EMSA for detection of NF-κB–DNA and ATF-4–DNA binding (35).

Human breast clinical specimen analysis. Human breast tumor specimens of different grades and normal breast tissues were collected from local hospital with informed consent and flash frozen. The levels of OPN and VEGF were examined by Western blot. The tumor sections were stained with H&E. The vWF expression and microvessel density were detected by immunofluorescence using anti-vWF antibody. To examine the status of NF-κB localization and NRP-1, Brk, and ATF-4 expressions, tumor tissue sections were analyzed by immunohistochemistry using their specific antibodies and were visualized under confocal microscopy (Zeiss).

Statistical analysis. The results of the experimental studies are expressed as mean ± SE. Statistical differences were analyzed by Student's *t* test. $P < 0.05$ was regarded as significant. All these bands were analyzed densitometrically (Kodak Digital Science), and the fold changes were calculated. The *in vivo* angiogenesis and all other *in vivo* experimental data were quantified using the Image Pro Plus 6.0 Software (Nikon).

Results

OPN augments the expression of VEGF. To examine whether OPN regulates VEGF expression and control breast tumor angiogenesis, MDA-MB-231 cells were treated with exogenous OPN, and VEGF expression were analyzed by Western blot (Fig. 1*A*) and by RT-PCR (Fig. 1*B*). The results indicated that OPN induces VEGF expression both at protein and RNA levels. To examine the specificity of OPN on VEGF expression, cells were individually

transfected with OPN cDNA or OPNi or treated with anti-OPN blocking antibody (R&D Systems). The data revealed that cells transfected with OPN cDNA enhanced, whereas transfected with OPNi or treated with anti-OPN antibody suppressed, the VEGF expression (Fig. 1*C*). To examine whether OPN regulates VEGF promoter activity, cells were individually transfected with OPN cDNA or OPNi along with VEGF-luciferase reporter construct. Cell lysates were analyzed by Western blot using antiluciferase antibody. The data showed that silencing of OPN drastically suppressed, whereas overexpression significantly enhanced, VEGF promoter activity (Fig. 1*D*). These results suggested that exogenous, as well as tumor-derived, OPN augments VEGF expression both at transcriptional and protein levels.

OPN stimulates Brk/NIK-dependent NF-κB activation. Brk is considered as one of the key regulator during breast cancer progression and is expressed moderately in MDA-MB-231 cells (22–24). We sought to determine whether OPN regulates Brk phosphorylation in MDA-MB-231 cells. Accordingly, cells were treated with OPN for 0 to 24 min, and level of pBrk was detected by immunoprecipitation followed by Western blot. The results showed that OPN enhances Brk phosphorylation (Supplementary Fig. S1*A*). Pretreatment of cells with αvβ3 blocking antibody significantly suppressed, whereas inhibitor of c-Src (pp2) or phosphatidylinositol 3-kinase (PI3K; wortmannin) had no effect on OPN-induced Brk phosphorylation and Brk kinase activation (Fig. 2*A*). The data are analyzed densitometrically and represented in the form of bar graph (Fig. 2*A*). Cells treated with RGD but not with RGE peptide also suppressed OPN-induced Brk phosphorylation (data not shown). These data suggested that OPN regulates αvβ3-integrin–dependent Brk activation, which is independent of c-Src/PI3K signaling pathway. Earlier, we have shown that NIK plays a crucial role in OPN-induced signaling, which in turn regulates tumor growth (18). To examine whether Brk plays any role on OPN-induced NIK phosphorylation, cells were individually transfected with wt or KM Brk and then treated with OPN. The data revealed that wt Brk enhanced, whereas KM Brk inhibited, OPN-induced NIK phosphorylation, indicating that Brk plays a crucial role in this process (Fig. 2*B*). EMSA results revealed that wt Brk enhanced, whereas KM Brk suppressed, OPN-induced NF-κB–DNA binding (Supplementary Fig. S1*B*). Moreover, Brk siRNA inhibited OPN-induced NF-κB–DNA binding (data not shown). These results define a novel-signaling pathway by which OPN regulates Brk-dependent NIK-mediated NF-κB activation.

OPN regulates crosstalk between NF-κB and ATF-4 leading to VEGF expression. Previous reports have indicated that ATF-4 regulates VEGF expression in response to various stimuli (26). To examine whether OPN regulates ATF-4 cellular localization, cells were treated with OPN or transfected with OPNi, and localization of ATF-4 was detected by immunofluorescence (Supplementary Fig. S1*C*). The results showed that OPN enhanced ATF-4 nuclear localization. To check whether OPN regulates ATF-4–DNA binding and involvement of Brk in this process, EMSA was performed. The data revealed that wt Brk enhanced, whereas KM Brk drastically suppressed, OPN-induced ATF-4–DNA binding (Fig. 2*C, lanes 1–4*). Brk siRNA also suppressed OPN-induced ATF-4–DNA binding (data not shown). IκBα sup. rep. or mut NIK inhibited, whereas wt NIK significantly enhanced, OPN-induced ATF-4–DNA binding (Fig. 2*C, lanes 5–9*). Cotransfection of cells with wt Brk along with IκBα sup. rep. or mut NIK unaffected OPN-induced ATF-4–DNA binding (Fig. 2*C, lanes 10* and *12*). Similar results were obtained

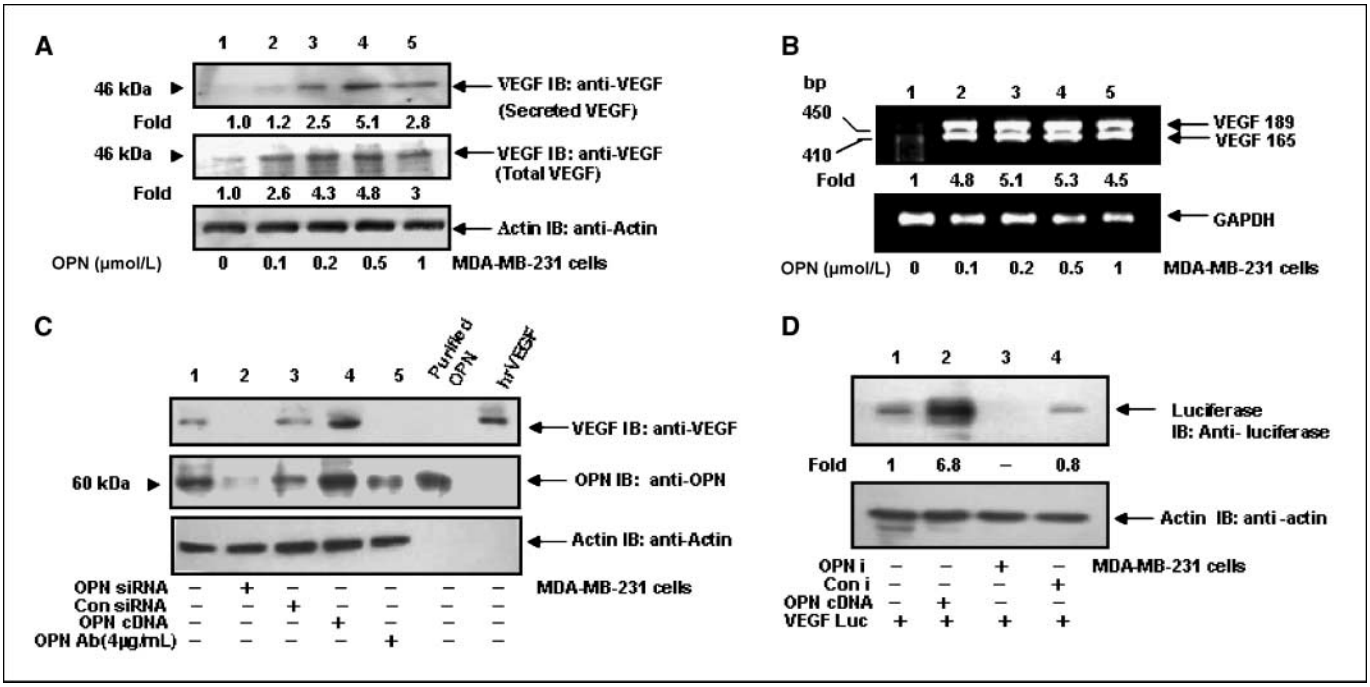

Figure 1. Exogenous and tumor-derived OPN augments VEGF expression in MDA-MD-231 cells. *A,* serum-starved cells were incubated with 0 to 1 μmol/L OPN for 6 h at 37°C, and conditioned media and cell lysates were analyzed by Western blot using anti-VEGF antibody. Actin was used as loading control. *B,* cells were treated with 0 to 1 μmol/L OPN for 3 h, total RNA was isolated, and the level of VEGF mRNA was detected by semiquantitative RT-PCR. Glyceraldehyde-3-phosphate dehydrogenase (*GAPDH*) was used as internal control. *C,* cells were transfected with OPN cDNA, OPNi, or Coni or treated with OPN blocking antibody. The expressions of VEGF and OPN in cell lysates were analyzed by Western blot using their specific antibodies. Human recombinant VEGF and purified OPN were used as controls. *D,* cells were transfected with VEGF-luciferase reporter construct alone or cotransfected with OPNi, Coni, or OPN cDNA, and luciferase expression was detected by Western blot using antiluciferase antibody. The data represent three experiments exhibiting similar results. Fold changes were calculated.

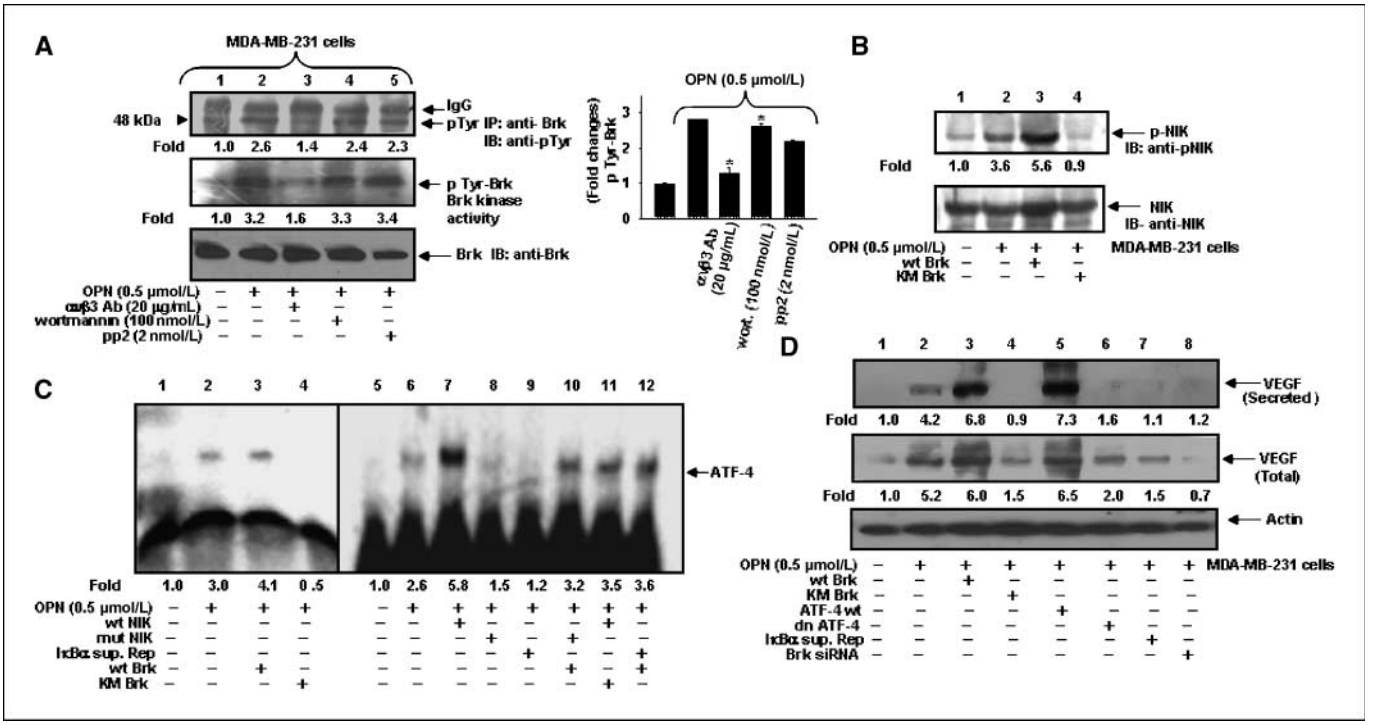

Figure 2. OPN regulates VEGF expression via Brk/NF-κB/ATF-4 signaling pathways in MDA-MB-231 cells. *A,* OPN induces Brk phosphorylation and kinase activity through αvβ3 integrin–dependent but c-Src and PI3K-independent pathway. Cells were treated with 0.5 μmol/L OPN for 8 min or pretreated with anti-αvβ3 antibody or wortmannin or pp2 for 2 h and then treated with OPN. The cell lysate was immunoprecipitated with anti-Brk antibody. Half of the immunoprecipitated samples were analyzed by Western blot using antiphosphotyrosine antibody. Remaining half of the samples was used for detecting Brk kinase activity by autophosphorylation study. Total Brk expression in the cells was used as loading control. The levels of p-Tyr-Brk were quantified by densitometric analysis and represented in the form of bar graph (*, $P < 0.03$). *B,* OPN-induced Brk-mediated NIK phosphorylation was determined by transfecting the cells with wt or KM Brk and then treated with 0.5 μmol/L OPN for 15 min. Cell lysates were analyzed by Western blot using anti–phosphorylated NIK antibody. *C,* Brk regulates OPN-dependent ATF-4–DNA binding and crosstalk between NF-κB and ATF-4. Cells were transfected with wt or KM Brk and treated with OPN. In separate experiments, cells were transfected with wt NIK or mut NIK or sup. rep. IκBα or wt Brk and mut NIK or KM Brk and wt NIK or wt Brk and IκBα sup. rep followed by treatment with OPN. ATF-4–DNA binding activity was analyzed by EMSA. Note that Brk up-regulates ATF-4 activity through NF-κB–dependent/independent pathway. *D,* roles of Brk and ATF-4 in OPN-induced VEGF expression. Cells were individually transfected with wt and KM Brk or wt and dn ATF-4 or Brk siRNA or IκBα sup. rep. and then treated with OPN. VEGF expressions (secreted and total) were analyzed by Western blot. All figures are representation of three experiments. Fold changes were calculated.

when cells were cotransfected with KM Brk along with wt NIK (Fig. 2*C, lane 11*). These data indicated that OPN up-regulates Brk-dependent ATF-4 activation. However, OPN also enhances Brk-dependent NIK/NF-κB–mediated ATF-4 activation. Transfection of cells with wt or dn ATF-4 had no effect on OPN-induced NF-κB–DNA binding, indicating that OPN-regulated crosstalk between NF-κB and ATF-4 is unidirectional toward ATF-4 (Supplementary Fig. S1*D*). To determine the role of Brk and ATF-4 on OPN-induced VEGF expression, cells were individually transfected with wt/KM Brk, Brk siRNA, or wt/dn ATF-4 and then treated with OPN. The results showed that cells transfected with wt Brk or wt ATF-4 increased VEGF expression upon OPN treatment, whereas transfection with KM Brk, Brk siRNA or dn ATF-4 showed drastic suppression of VEGF expression (Fig. 2*D*). Moreover, IκBα sup. rep. significantly reduced OPN-induced VEGF expression (Fig. 2*D*). The effect of OPN on VEGF promoter activity was examined either by transfecting the cells with VEGF-GFP reporter construct alone or cotransfecting with wt and KM Brk, wt and dn ATF-4, IκBα sup. rep., or Brk siRNA and then treated with OPN. The OPN-induced GFP expression was analyzed by fluorescence microscopy (Nikon), quantified by Image Pro Plus 6.0 Software (Nikon), and represented in the form of bar graph (Supplementary Fig. S2). These data clearly suggested that Brk, ATF-4, and NF-κB play important role in OPN-induced VEGF expression both at transcriptional and protein level.

VEGF and its receptor NRP-1 play crucial roles in OPN-regulated breast tumor cell motility through autocrine mechanism. Recent data revealed that VEGF acts as survival, migratory and proliferative factor in breast carcinoma cells (10, 36). NRP-1 is the only VEGF-specific receptor that is expressed in MDA-MB-231 cells (29, 30). We therefore speculated that OPN might regulate the interaction between VEGF and NRP-1, which may control the motility of MDA-MB-231 cells. Accordingly, cells were treated with OPN alone or along with anti-VEGF or anti-NRP-1 blocking antibody, and lysates were immunoprecipitated with anti-VEGF antibody and immunoblotted with anti–NRP-1 antibody. The data suggested that OPN-induced VEGF interacts with NRP-1 in MDA-MB-231 cells through autocrine manner (Fig. 3*A, I*). To examine whether OPN has any effect on breast tumor cell motility and whether VEGF and NRP-1 are involved in this process, wound assay was performed using MDA-MB-231 cells with typical cobblestone morphology. Wounds with a constant diameter were made, and cells were treated with OPN alone or along with anti-VEGF or anti–NRP-1 blocking antibody. In separate experiments, cells were transfected with NRP-1i and then treated with OPN, and wound assay was performed. The wound photographs were taken under phase contrast microscope (Fig. 3*A, II*). Moreover, cells transfected with wt Brk or wt ATF-4 enhanced, whereas KM Brk or dn ATF-4 drastically suppressed, OPN-induced wound migration

(Fig. 3*A, II*). Interestingly, the enhanced wound migration caused by overexpression of wt Brk or wt ATF-4 was suppressed upon treatment of cells with anti-VEGF and anti–NRP-1 blocking antibodies (Fig. 3*A, II*). These results clearly indicated that OPN regulates VEGF-dependent wound migration through NRP-1–mediated autocrine mechanism.

OPN-induced VEGF controls KDR-dependent endothelial cell motility and *in vivo* angiogenesis through paracrine and juxtacrine mechanisms. Tumor-derived VEGF interacts with endothelial cell surface VEGF receptor-2 (also called KDR) and induces KDR phosphorylation that leads to tumor angiogenesis (37). Therefore, we sought to determine whether OPN-induced VEGF, which is expressed in MDA-MB-231 cells, can regulate KDR phosphorylation in endothelial (EA.hy-926) cell line through paracrine loop. Accordingly, MDA-MB-231 cells were treated with OPN and CM either alone or mixed with anti-VEGF blocking antibody incubated with endothelial cells. In separate experiments, CM of OPNi transfected MDA-MB-231 cells were incubated with endothelial cells. Cell lysates were analyzed by Western blot for KDR phosphorylation. The data revealed that OPN-induced VEGF enhanced KDR phosphorylation in endothelial cells through paracrine mechanism (Supplementary Fig. S3*A*). To investigate whether OPN-induced MDA-MB-231 cell-derived VEGF regulates endothelial cell wound motility, MDA-MB-231 cells were either

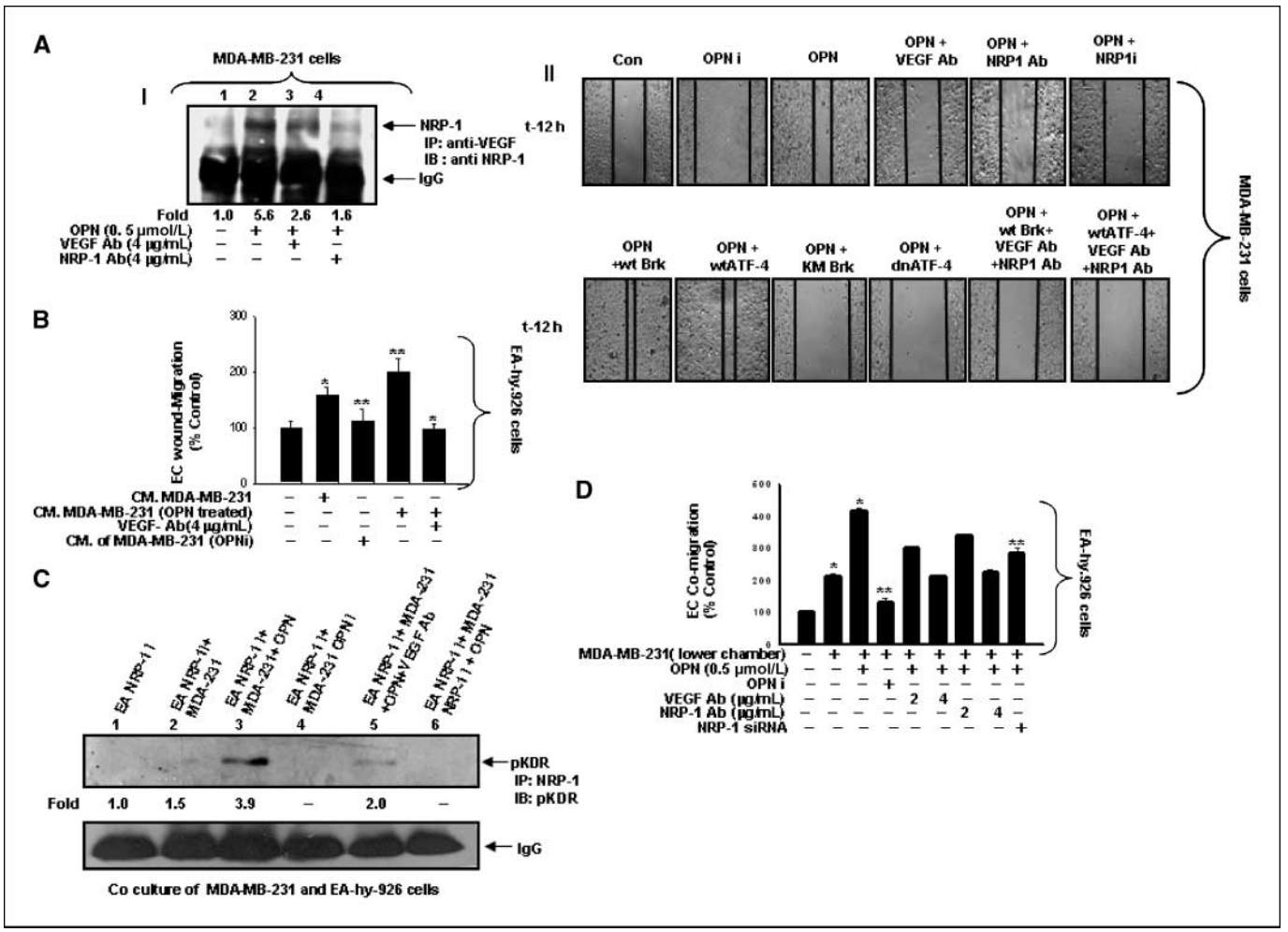

Figure 3. *A,* OPN enhances the VEGF–NRP-1 interaction in MDA-MB-231 cells. *I,* OPN-induced VEGF–NRP-1 interactions were examined by treating the cells with OPN for 6 h or pretreated with anti-VEGF or anti–NRP-1 blocking antibody and then treated with OPN. Cell lysates were immunoprecipitated with anti-VEGF antibody and analyzed by Western blot with anti–NRP-1 antibody. *II,* VEGF and NRP-1 play crucial roles in OPN-induced tumor cell motility. Wounds with a constant diameter were made, and cells were treated with OPN. In separate experiments, cells were transfected with wt and KM Brk or wt and dn ATF-4 and then treated with OPN in absence or presence of anti-VEGF or anti–NRP-1 blocking antibody, and wound assay was performed. In separate experiments, cells were individually transfected with OPNi, and wound assay was conducted. Cells were also transfected with NRP-1i and then treated with OPN. Wound photographs were taken after termination of the experiments (t = 12 h). *B,* OPN controls VEGF-dependent endothelial cell (*EC*) wound migration in a paracrine mechanism. Endothelial (EA-hy.926) cells were incubated with conditioned media obtained from OPN-treated or OPNi transfected MDA-MB-231 cells, and wound assay was performed and represented in the form of bar graph (*, $P < 0.007$; **, $P < 0.01$). In separate experiments, endothelial cells were also incubated with OPN-treated conditioned media mixed with anti-VEGF blocking antibody and used for wound assay. *C,* OPN enhances VEGF-dependent NRP-1/pKDR mediated tumor-endothelial cell interaction through juxtacrine mechanism. Endothelial cells were transfected with NRP-1i (EA NRP-1i) and cocultured with normal or OPNi or NRP-1i transfected MDA-MB-231 cells. OPN alone or along with anti-VEGF blocking antibody were added to the cocultured cells. Cell lysates were immunoprecipitated with anti–NRP-1 antibody and analyzed by Western blot with anti–phosphorylated KDR antibody. *D,* OPN enhances VEGF/NRP-1–mediated endothelial cell migration through juxtacrine manner. Endothelial cells were added on the upper portion of modified Boyden chamber. MDA-MB-231 cells seeded in lower chamber were either treated with OPN alone or along with anti-VEGF or anti–NRP-1 blocking antibody and used for direct comigration assays. In separate experiments, MDA-MB-231 cells were transfected with OPNi or NRP-1i and seeded in the lower chamber, and comigration assays were performed. Endothelial cells were migrated from upper chamber to the lower chamber and counted under inverted microscope (Nikon). *Columns,* means of three determinations; *bars,* SE (*, $P < 0.001$; **, $P < 0.004$).

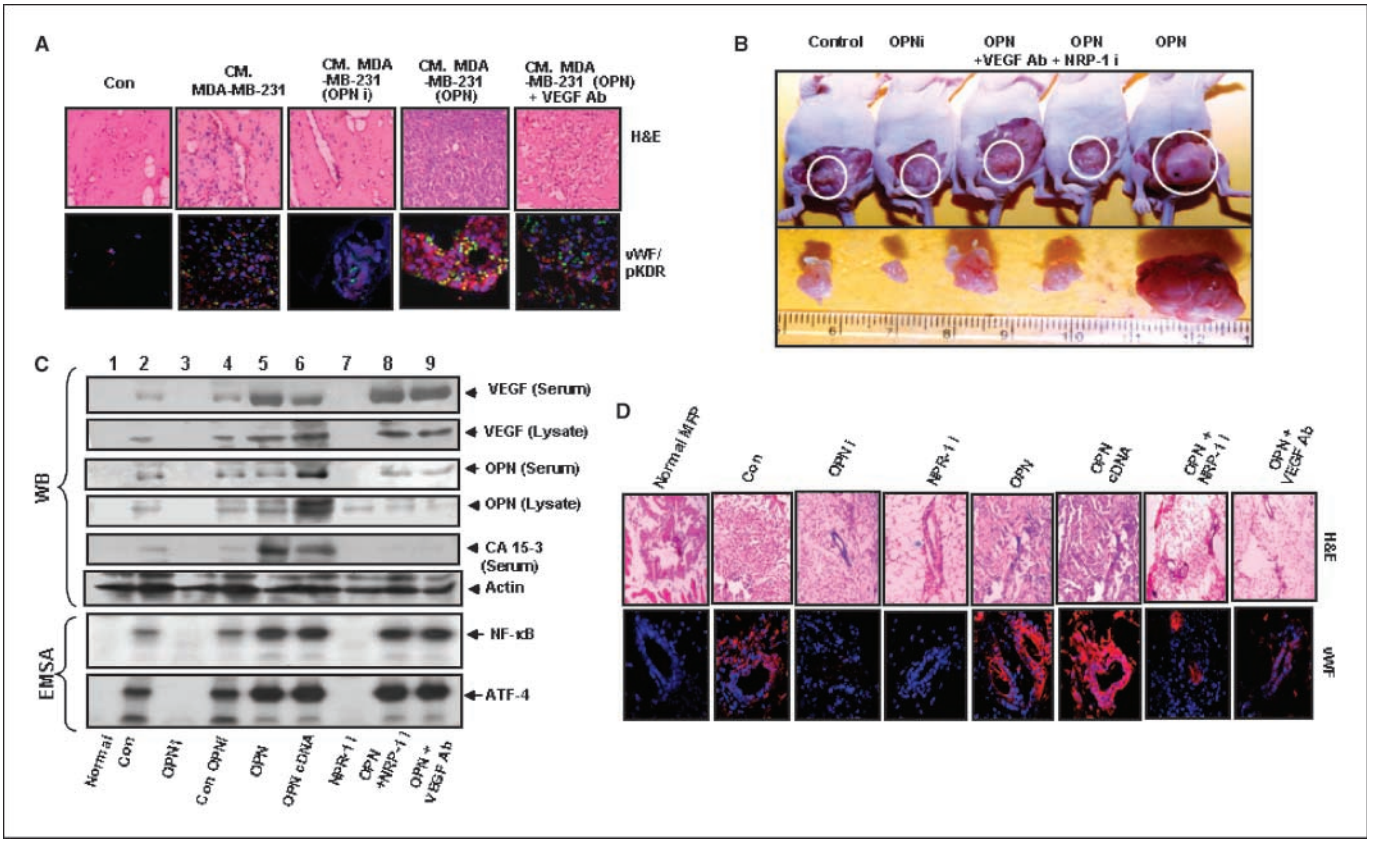

Figure 4. OPN induces VEGF/NRP-1–dependent tumor growth and angiogenesis in nude mice model. *A,* OPN regulates VEGF-dependent angiogenesis in Matrigel plug assay. The OPNi-transfected or OPN-treated CM of MDA-MB-231 cells either alone or along with anti-VEGF antibody were mixed with Matrigel and then injected s.c. to ventral groin region of nude mice (NMRI, nu/nu). Matrigel plugs were excised, and the sections were subjected to histopathologic analysis. Note that endothelial cell nuclei stained blue were observed inside the bed of pink stained Matrigel. The endothelial cells were further characterized by immunofluorescence using anti-vWF antibody (stained with Cy3; *red*) as marker and visualized under confocal microscopy. The phosphorylation of KDR was also detected by immunofluoresence by using anti–phosphorylated KDR antibody followed by staining with FITC (*green*). Nuclei were stained with 4′,6-diamidino-2-phenylindole (DAPI; *blue*). *B,* typical photographs of orthotopic breast tumors in athymic nude mice model. *Bottom,* excised tumors of respective mice. Six mice were used in each set of experiments. *C,* the levels of VEGF, OPN, and CA 15-3 from xenograft tumor lysates and sera were analyzed by Western blot. NF-κB and ATF-4–DNA-binding in these orthotopic tumors were analyzed by EMSA. Actin was used as control. *D,* mice breast tumors were analyzed by histopathology (*top*) and immunohistochemistry using anti-vWF antibody (*bottom*). vWF was stained with Cy3 (*red*) and nuclei were counterstained with DAPI (*blue*). Normal mammary fat pad (*MFP*) is used as control.

treated or transfected under similar conditions as described above and endothelial cell wound migration was performed. The data are analyzed and represented in the form of bar graph (Fig. 3*B*). These results showed that OPN enhances VEGF-dependent endothelial cell motility in paracrine mechanism.

The interaction of OPN-induced VEGF with NRP-1 and KDR through juxtacrine mechanism is shown by coculture experiments using MDA-MB-231 and endothelial cells. Accordingly, endothelial cells were transfected with NRP-1i and cocultured with MDA-MB-231 cells in the presence of OPN alone or along with anti-VEGF antibody. In separate experiments, MDA-MB-231 cells were also transfected with OPNi or NRP-1i and used for coculture experiments. The cell lysates were immunoprecipitated with anti–NRP-1 antibody, followed by immunoblotting with anti–pKDR antibody. Our data revealed that OPN-induced VEGF acts as bridge between NRP-1, expressed in tumor cells, and KDR, expressed in endothelial cells, and regulates NRP-1–mediated KDR phosphorylation through juxtacrine mechanism (Fig. 3*C*). To verify whether pKDR is indeed expressed in endothelial but not in MDA-MB-231 cells, endothelial cells were incubated with CM of OPN-treated MDA-MB-231 cells. In separate experiments, MDA-MB-231 cells were also treated with OPN. The level of pKDR was analyzed by Western blot. The results showed that pKDR/KDR is detectable only in endothelial but not in MDA-MB-231 cells (Supplementary Fig. S3*B*). The endothelial-breast tumor cell interaction was further examined by direct comigration assay. The MDA-MB-231 cells either treated with exogenous OPN or transfected with OPNi or NRP-1i or treated with anti-VEGF or anti–NRP-1 antibody followed by treatment with OPN and used in the lower chamber whereas endothelial cells were used in the upper portion of modified Boyden chamber. The results showed that OPN stimulates VEGF/NRP-1–mediated endothelial cell migration through juxtacrine pathway (Fig. 3*D*). Taken together, these data showed that OPN-induced VEGF interacts with endothelial cell surface receptor, KDR, and regulates endothelial cell motility through paracrine and juxtacrine mechanisms.

OPN promotes VEGF-dependent *in vivo* angiogenesis. To assess whether OPN regulates VEGF-dependent *in vivo* angiogenesis, Matrigel plug assay was performed. The CM obtained from OPN-treated or OPNi-transfected MDA-MB-231 cells was mixed with Matrigel either alone or along with anti-VEGF blocking antibody and injected s.c. (ventral groin region) to the nude mice. Matrigel plugs were excised, and the sections were analyzed by

histopathologic and immunohistochemical studies using anti-vWF and anti-pKDR antibodies. The data revealed that OPN enhances VEGF-dependent *in vivo* angiogenesis through KDR phosphorylation (Fig. 4*A*). The neovascularization and KDR phosphorylation were quantified and represented graphically (Supplementary Fig. S4*A*). The data showed that OPN regulates VEGF-dependent *in vivo* angiogenesis through paracrine loop, whereas silencing tumor-derived OPN resulted in drastic reduction of tumor angiogenesis.

VEGF plays a crucial role in OPN-induced tumor growth and angiogenesis in orthotopic mice model. Our *in vitro* and *in vivo* data prompted us to examine whether OPN regulates tumor growth in orthotopic nude mice model and whether VEGF is involved in this process. Accordingly, MDA-MB-231 cells were transfected with OPN cDNA or treated with OPN and injected orthotopically into the mammary fat pad of female nude mice. In separate experiments, OPNi or NRP-1i were mixed with transfection reagent and injected to the site of the tumor. Purified OPN and anti-VEGF blocking antibody were injected intratumorally twice a week up to completion of the experiments. After 6 weeks, mice were sacrificed and tumors were collected. The typical photographs of tumors are shown in Fig. 4*B*. The changes of tumor weight (% to control) were analyzed and represented as bar graph (Supplementary Fig. S4*B*). Blocking of VEGF with its antibody or NRP-1i significantly suppressed OPN-induced breast tumor growth in nude mice suggesting that VEGF and its receptor NRP-1 play crucial role in this process.

Tumor sections were also analyzed by histopathology. The results showed that tumors generated by OPN exhibit enhanced tumor cell infiltration, poor differentiation, higher nuclear polymorphism, mitotic count (12–16/hpf) and increased vessel formation in mammary fat pad of mice compared with control (Fig. 4*D, top*). Moreover, well-differentiated tumor structure, little infiltration and nuclear polymorphism, lesser mitotic features (2-5/hpf), and decreased vessel formation were observed in the tumors of the mice injected with anti-VEGF blocking antibody or NRP-1i along with OPN. To examine whether OPN regulates tumor angiogenesis, mice tumors were analyzed by immunohistochemistry using anti-vWF antibody (Fig. 4*D, bottom*; Supplementary Fig. S4*C*). The results indicated that OPN enhanced microvessel density, whereas blocking of VEGF or silencing NRP-1 suppressed OPN-induced tumor angiogenesis. Silencing tumor-derived OPN drastically suppressed vWF expression, suggesting the potential role of tumor-derived OPN in tumor angiogenesis. To examine

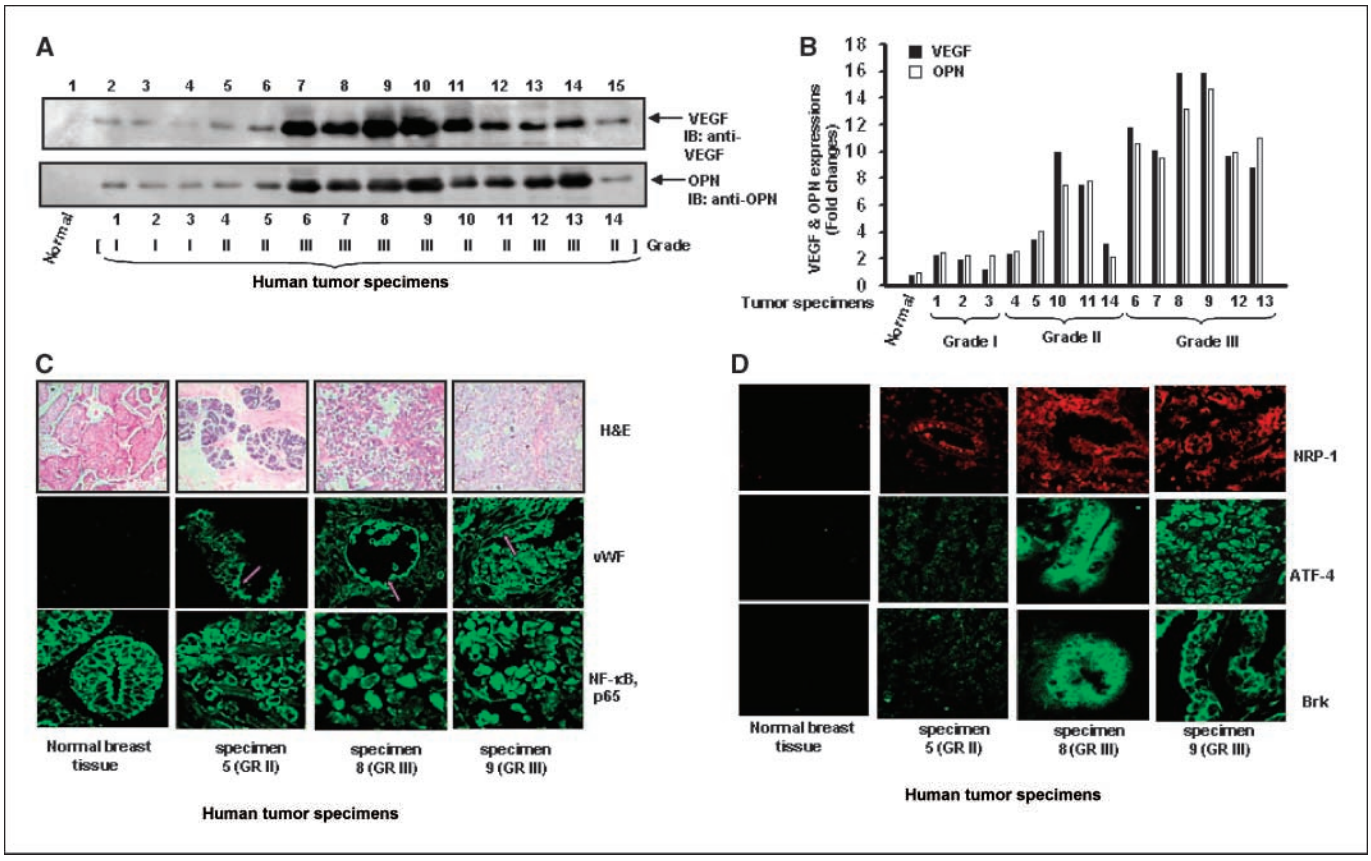

Figure 5. *A* and *B,* analysis of human breast tumor clinical specimens with different pathologic grades. Human breast tumor specimens (1–14) were collected from local hospital with informed consent. The tumor grading was performed by histopathologic analysis using a modified Scarff-Bloom-Richardson system. Tumor samples were analyzed by Western blot using anti-VEGF or anti-OPN antibody (*A*). The levels of OPN and VEGF were also detected in normal breast epithelial tissues. The expressions of OPN and VEGF were quantified and represented in the form of bar graph (*B*). *C* and *D,* histopathologic micrographs of normal and breast tumor tissues of different grades (specimen 5, grade II; specimens 8 and 9, grade III). The sections of normal and tumor tissues (specimens 5, 8, and 9) of different grades were analyzed by immunohistochemistry using anti-vWF antibody. Note that the enhanced microvessel density was observed in higher grades of tumor (specimens 8 and 9) and correlates with increased OPN and VEGF expressions. The vWF-positive areas indicate the microvessel density (*pink arrows*). Cellular localization of NF-κB and expression profiles of NRP-1, ATF-4, and Brk were analyzed by immunohistochemical studies using their specific antibodies. Note that NF-κB, ATF-4, and Brk are stained with FITC (*green*), whereas NRP-1 is stained with TRITC (*red*).

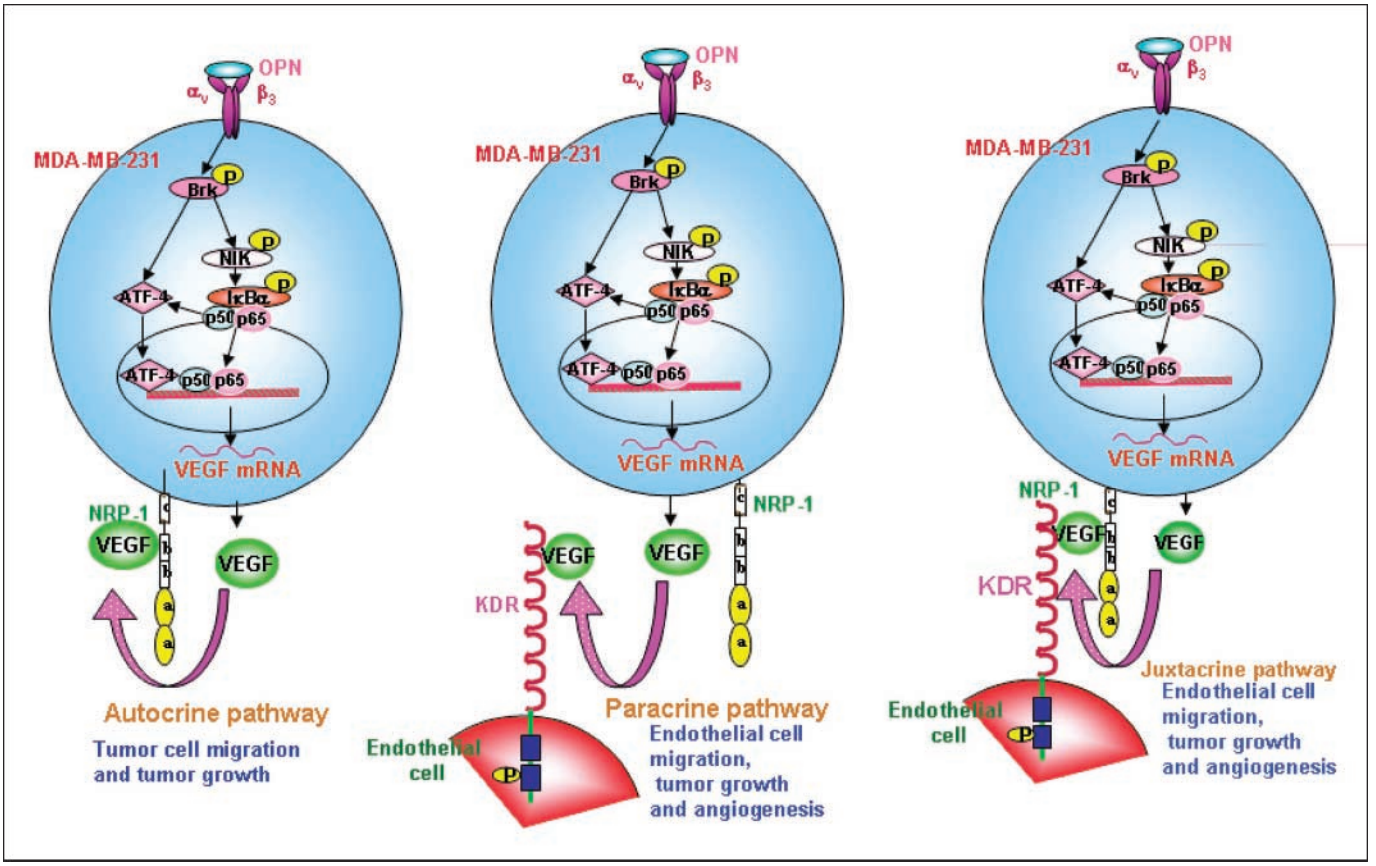

Figure 6. A schematic representation of OPN-induced NF-κB/ATF-4–mediated VEGF expression through activation of Brk/NIK leading to tumor growth and angiogenesis through autocrine, paracrine, and juxtacrine mechanisms.

whether OPN enhances the interaction between VEGF and NRP-1 *in vivo* system, the tumor lysates were immunoprecipitated with anti-VEGF antibody and analyzed by Western blot using anti–NRP-1 antibody. Treatment with anti-VEGF blocking antibody or silencing NRP-1 significantly suppressed OPN-induced interaction between VEGF and NRP-1 (data not shown) and further suggested that OPN augments the interaction between VEGF and NRP-1 that ultimately control the tumor growth and angiogenesis.

Tumor tissues were lysed, and the levels of OPN and VEGF were detected by Western blot (Fig. 4*C*). The level of CA15-3 from mice serum was analyzed as breast cancer marker. The levels of VEGF and OPN were also detected from mice serum (Fig. 4*C*). Significant induction of VEGF was observed in tumor generated by OPN. Tumor samples were also analyzed by EMSA (Fig. 4*C*) and immunofluorescence (Supplementary Fig. S4*D*), and the data suggested that OPN augments NF-κB and ATF-4–DNA binding and nuclear localization in these tumors. Moreover, silencing tumor-derived OPN significantly suppressed NF-κB and ATF-4–DNA binding and nuclear localization. These data suggested that both tumor-derived and exogeneous OPN regulates NF-κB and ATF-4–dependent VEGF/NRP-1–mediated breast tumor progression and angiogenesis.

Expressions of OPN and VEGF and their implications in human breast tumor angiogenesis. The *in vitro* and *in vivo* data further prompted us to extend these studies in human clinical breast tumor specimens. Human solid breast tumor specimens and regional lymph nodes were collected with informed consent from a local hospital. Tumor grading was performed with the help of expert oncopathologist using modified Scarff-Bloom-Richardson system, and regional lymph node metastasis was analyzed by histopathology (Supplementary Table S1). The expressions of OPN and VEGF (Fig. 5*A*) and the interaction between VEGF and NRP-1 (data not shown) were studied in tumor specimens of different grades. The levels of OPN and VEGF were quantified and represented as bar graph (Fig. 5*B*). The data revealed that there were significantly higher levels of OPN and VEGF expressions (Fig. 5*A*; 8 of 14 tumor specimens and one normal sample), and these data correlated with tumors of higher grades. The data also indicated that the interaction between VEGF and NRP-1 was also enhanced significantly with tumors of higher grades (data not shown). The immunohistochemical staining with anti-vWF antibody showed the enhanced angiogenic vessel formation in breast tumor specimens of higher grades (Fig. 5*C*).

Localization and expression of NF-κB, ATF-4, Brk, and NRP-1 in breast tumors specimens. To examine the activation status of NF-κB in different grades of tumor specimens, tissue sections were analyzed by immunohistochemistry using anti–NF-κB, p65 antibody. The results indicated that the NF-κB nuclear localization was significantly enhanced in higher grades (grades II and III) of tumors compared with the tumor of lower grades or normal breast tissues (Fig. 5*C*). The status of expressions of NRP-1, ATF-4, and Brk in different grades of tumors was also analyzed by immunohistochemistry using their specific antibodies. These results indicated that the higher expressions of NRP-1, ATF-4, and Brk correlate with higher grades of tumors (Fig. 5*D*). The ATF-4 nuclear

localization was also significantly enhanced in higher grades (grades II and III) of tumors and correlated with NF-κB (Fig. 5*C* and *D*). The status of OPN and VEGF expressions and its correlation with NF-κB and ATF-4 activation and metastatic potential in various grades of tumors are summarized in Supplementary Table S1. These results showed that tumors with higher grades exhibit significantly higher levels of ATF-4 and NF-κB nuclear localization, and these data correlated with enhanced OPN, Brk, and VEGF expression both in *in vitro* and *in vivo* systems, which further corroborated with tumor growth and angiogenesis in breast carcinoma.

Discussion

We have for the first time shown the molecular mechanism of OPN-induced VEGF expression and its potential role in regulating *in vitro* cell motility which ultimately modulates *in vivo* tumor growth and angiogenesis in breast cancer model. Our data also revealed that OPN might be necessary for maximal induction of neovascularization by inducing VEGF expression through activation of Brk/NF-κB/ATF-4 pathways. Several lines of evidences support this conclusion. First, OPN regulates VEGF promoter activity and expression in human breast carcinoma cell lines. Second, OPN stimulates Brk phosphorylation and Brk/NIK-mediated NF-κB–dependent/independent ATF-4 activation and crosstalk between NF-κB and ATF-4 that leads to VEGF expression. Third, in autocrine pathway, OPN-induced VEGF interacts with tumor cell surface receptor NRP-1 and stimulates VEGF–NRP-1–mediated tumor cell motility. Fourth, in paracrine loop, OPN-induced VEGF up-regulates KDR phosphorylation, resulting in enhanced endothelial cell motility and *in vivo* angiogenesis in nude mice. Fifth, in juxtacrine manner, OPN-induced VEGF regulates tumor-endothelial cell interaction through binding with NRP-1 in breast cancer and KDR in endothelial cells. Sixth, OPN-induced VEGF leads to increased breast tumor growth and angiogenesis in nude mice model and blocking of tumor-derived VEGF or silencing of tumor-derived OPN and NRP-1 significantly suppressed breast tumor progression and angiogenesis. Seventh, analysis of human solid breast tumor specimens showed the significant correlation between the OPN, Brk, NRP-1, and VEGF expressions NF-κB and ATF-4 activations with different pathologic grades of tumors. All these data supported by the fact that OPN and its downstream signaling molecules might be used as therapeutic target for the treatment of breast cancer.

Previous reports indicated that Brk plays important role during breast tumor progression (22, 23). We provide evidence, at least in part, that Brk plays crucial role in OPN-induced NIK-mediated NF-κB activation. Our data also showed that OPN regulates Brk-dependent ATF-4 activation and a crosstalk between NF-κB and ATF-4 that controls VEGF-dependent tumor angiogenesis. NRP-1 acts as key receptor for VEGF-mediated signaling in MDA-MB-231 cells (36, 38). Recent evidence indicated that NRP-1 could independently regulate VEGF-induced cell signaling (39). We sought to determine whether OPN plays any role in regulating the interaction between VEGF and NRP-1 in breast cancer cells. Our results showed that enhanced interaction of VEGF and NRP-1 in response to OPN control the breast cancer cell migration and tumor growth through autocrine mechanism. We have also shown that OPN-induced tumor-derived VEGF regulates KDR/NRP-1–mediated endothelial cell motility and tumor angiogenesis through paracrine and juxtacrine mechanisms.

The role of OPN in the regulation of tumor angiogenesis is under intense investigation (12, 40). Earlier Senger et al. reported that VEGF induces OPN expression in endothelial cells, which in turn regulates angiogenesis (41). However we have shown that OPN regulates VEGF expression, which controls tumor angiogenesis through autocrine, paracrine, and juxtacrine pathways. These data suggested that there could be a positive feedback loop between OPN and VEGF which might play an important role in tumor progression and angiogenesis. It has also been reported that coexpression of VEGF and OPN correlates with angiogenesis in patients with stage I lung adenocarcinoma (42). Earlier reports have shown that cooperation of OPN and VEGF may facilitate tumor progression and angiogenesis in carcinomas derived from other organs (43). Recently, we have showed that OPN regulates cyclooxygenase-2–dependent prostaglandin E_2 production, which in turn regulates prostate cancer angiogenesis (14). Although earlier reports indicated that OPN acts as an angiogenic factor but the molecular mechanism by which OPN regulates VEGF-dependent tumor angiogenesis in breast cancer is not well defined. Our study for the first time showed the in-depth signaling pathways by which OPN induces cell migration and angiogenesis through induction of VEGF expression in breast cancer. Moreover, these studies correlate with the data obtained from human breast tumor specimens in Indian scenario.

Suppression of tumor progression by targeting the angiogenic switch is one of the greatest challenges for cancer biologists and medical oncologists. Recent reports on anticancer therapy indicated that suppression of tumor angiogenesis by administration of antiangiogenic molecules is one of the most potent therapeutic approaches for the treatment of cancer (44). However, it is also known that some side effect of these antiangiogenic drugs are considered as the main problem of this therapy (45). Faced with the barrier to the traditional antiangiogenic strategies, we tested an *in vivo* RNA interference–based approach by targeting OPN and NRP-1. In recent time, *in vivo* siRNA-based approach has been proposed for treatment of several diseases including cancer (46). Therefore, appropriately designed OPN siRNA, injected intratumorally, exhibit significant suppression of tumor angiogenesis and may help in the surgical excision of tumor and provide considerable therapeutic value for the treatment of cancer.

Finally, we have shown for the first time that OPN induced the potent angiogenic molecule, VEGF expression. OPN regulates tumor growth and angiogenesis by induction of VEGF expression through activation of Brk/NF-κB/ATF-4 pathways. These data showed that OPN-induced VEGF regulates tumor angiogenesis through autocrine, paracrine, and juxtacrine mechanisms (Fig. 6). Our results further warrant that the mechanism shown in the mouse model underlies the human pathology, and a clear understanding of such mechanism(s) may facilitate the development of novel therapeutic approaches to suppress OPN-regulated NF-κB/ATF-4–dependent VEGF expression, thereby controlling tumor growth and angiogenesis.

Acknowledgments

Received 6/12/2007; revised 10/5/2007; accepted 10/29/2007.

Grant support: Department of Biotechnology, Government of India (G.C. Kundu) and Council of Scientific and Industrial Research, Government of India (G. Chakraborty and S. Jain).

The costs of publication of this article were defrayed in part by the payment of page charges. This article must therefore be hereby marked *advertisement* in accordance with 18 U.S.C. Section 1734 solely to indicate this fact.

References

1. Folkman J, Shing Y. Angiogenesis. J Biol Chem 1992; 267:10931–4.
2. Rifkin DB, Moscatelli D. Recent developments in the cell biology of basic fibroblast growth factor. J Cell Biol 1989;109:1–6.
3. Nicosia RF, Nicosia SV, Smith M. Vascular endothelial growth factor, platelet-derived growth factor, and insulin-like growth factor-1 promote rat aortic angiogenesis *in vitro*. Am J Pathol 1994;145:1023–9.
4. Gleave ME, Hsieh JT, Wu HC, et al. Epidermal growth factor receptor-mediated autocrine and paracrine stimulation of human transitional cell carcinoma. Cancer Res 1993;53:5300–7.
5. McMahon G. VEGF receptor signaling in tumor angiogenesis. Oncologist 2000;5:3–10.
6. Ferrara N. VEGF and the quest for tumor angiogenesis factors. Nat Rev Cancer 2002;2:795–803.
7. Ferrara N, Gerber HP, LeCouter J. The biology of VEGF and its receptors. Nat Med 2003;9:669–76.
8. Cross MJ, Dixelius J, Matsumoto T, Claesson-Welsh L. VEGF-receptor signal transduction. Trends Biochem Sci 2003;28:488–94.
9. Banerjee SN, Sengupta K, Banerjee S, Saxena NK, Banerjee SK. 2-Methoxyestradiol exhibits a biphasic effect on VEGF-A in tumor cells and upregulation is mediated through ER-α, a possible signaling pathway associated with the impact of 2-ME2 on proliferative cells. Neoplasia 2003;5:417–26.
10. Mercurio AM, Bachelder RE, Bates RC, Chung J. Autocrine signaling in carcinoma: VEGF and the α 6 β 4 integrin. Semin Cancer Biol 2004;14:115–22.
11. Sodek J, Ganss B, McKee MD. Osteopontin. Crit Rev Oral Biol Med 2000;11:279–303.
12. Chakraborty G, Jain S, Behera R, et al. The multifaceted roles of osteopontin in cell signaling, tumor progression and angiogenesis. Curr Mol Med 2006;6:819–30.
13. Wai PY, Kuo PC. The role of osteopontin in tumor metastasis. J Surg Res 2004;121:228–41.
14. Jain S, Chakraborty G, Kundu GC. The crucial role of cyclooxygenase-2 in osteopontin-induced protein kinase C α/c-Src/IκB kinase α/β-dependent prostate tumor progression and angiogenesis. Cancer Res 2006;66: 6638–48.
15. Philip S, Bulbule A, Kundu GC. Osteopontin stimulates tumor growth and activation of promatrix metalloproteinase-2 through nuclear factor-κ B-mediated induction of membrane type 1 matrix metalloproteinase in murine melanoma cells. J Biol Chem 2001;276: 44926–35.
16. Das R, Mahabeleshwar GH, Kundu GC. Osteopontin stimulates cell motility and nuclear factor κB-mediated secretion of urokinase type plasminogen activator through phosphatidylinositol 3-kinase/Akt signaling pathways in breast cancer cells. J Biol Chem 2003;278: 28593–606.
17. Rangaswami H, Bulbule A, Kundu GC. Nuclear factor-inducing kinase plays a crucial role in osteopontin-induced MAPK/I κ B α kinase-dependent nuclear factor κ B-mediated promatrix metalloproteinase-9 activation. J Biol Chem 2004;279:38921–35.
18. Rangaswami H, Bulbule A, Kundu GC. Osteopontin: role in cell signaling and cancer progression. Trends Cell Biol 2006;16:79–87.
19. Rittling SR, Chen Y, Feng F, Wu Y. Tumor-derived osteopontin is soluble, not matrix associated. J Biol Chem 2002;277:9175–82.
20. Senger DR, Perruzzi CA, Papadopoulos A, Tenen DG. Purification of a human milk protein closely similar to tumor-secreted phosphoproteins and osteopontin. Biochim Biophys Acta 1989;996:43–8.
21. Denhardt DT, Mistretta D, Chambers AF, et al. Transcriptional regulation of osteopontin and the metastatic phenotype: evidence for a Ras-activated enhancer in the human OPN promoter. Clin Exp Metastasis 2003;20:77–84.
22. Zhang P, Ostrander JH, Faivre EJ, Olsen A, Fitzsimmons D, Lange CA. Regulated association of protein kinase B/Akt with breast tumor kinase. J Biol Chem 2005;280:1982–91.
23. Chen HY, Shen CH, Tsai YT, Lin FC, Huang YP, Chen RH. Brk activates rac1 and promotes cell migration and invasion by phosphorylating paxillin. Mol Cell Biol 2004; 24:10558–72.
24. Harvey AJ, Crompton MR. Use of RNA interference to validate Brk as a novel therapeutic target in breast cancer: Brk promotes breast carcinoma cell proliferation. Oncogene 2003;22:5006–10.
25. Roybal CN, Yang S, Sun CW, et al. Homocysteine increases the expression of vascular endothelial growth factor by a mechanism involving endoplasmic reticulum stress and transcription factor ATF4. J Biol Chem 2004; 279:14844–52.
26. Roybal CN, Hunsaker LA, Barbash O, Vander Jagt DL, Abcouwer SF. The oxidative stressor arsenite activates vascular endothelial growth factor mRNA transcription by an ATF4-dependent mechanism. J Biol Chem 2005; 280:20331–9.
27. He Z, Tessier-Lavigne M. Neuropilin is a receptor for the axonal chemorepellent semaphorin III. Cell 1997;90: 739–51.
28. Kolodkin AL, Levengood DV, Rowe EG, Tai YT, Giger RJ, Ginty DD. Neuropilin is a semaphorin III receptor. Cell 1997;90:753–62.
29. Soker S, Fidder H, Neufeld G, Klagsbrun M. Characterization of novel vascular endothelial growth factor (VEGF) receptors on tumor cells that bind VEGF165 via its exon 7-encoded domain. J Biol Chem 1996;271:5761–7.
30. Soker S, Takashima S, Miao HQ, Neufeld G, Klagsbrun M. Neuropilin-1 is expressed by endothelial and tumor cells as an isoform-specific receptor for vascular endothelial growth factor. Cell 1998;92:735–45.
31. Miao HQ, Lee P, Lin H, Soker S, Klagsbrun M. Neuropilin-1 expression by tumor cells promotes tumor angiogenesis and progression. FASEB J 2000;14:2532–9.
32. Barr MP, Byrne AM, Duffy AM, et al. A peptide corresponding to the neuropilin-1-binding site on VEGF (165) induces apoptosis of neuropilin-1-expressing breast tumour cells. Br J Cancer 2005;92:328–33.
33. Leopold JA, Walker J, Scribner AW, et al. Glucose-6-phosphate dehydrogenase modulates vascular endothelial growth factor-mediated angiogenesis. J Biol Chem 2003;278:32100–6.
34. Sweeney CJ, Mehrotra S, Sadaria MR, et al. The sesquiterpene lactone parthenolide in combination with docetaxel reduces metastasis and improves survival in a xenograft model of breast cancer. Mol Cancer Ther 2005;4:1004–12.
35. Chakraborty G, Rangaswami H, Jain S, Kundu GC. Hypoxia regulates cross-talk between Syk and Lck leading to breast cancer progression and angiogenesis. J Biol Chem 2006;281:11322–31.
36. Bachelder RE, Crago A, Chung J, et al. Vascular endothelial growth factor is an autocrine survival factor for neuropilin-expressing breast carcinoma cells. Cancer Res 2001;61:5736–40.
37. Matsumoto T, Claesson-Welsh L. VEGF receptor signal transduction. Sci STKE 2001;RE 21:1–17.
38. Bachelder RE, Lipscomb EA, Lin X, et al. Competing autocrine pathways involving alternative neuropilin-1 ligands regulate chemotaxis of carcinoma cells. Cancer Res 2003;63:5230–3.
39. Wang L, Zeng H, Wang P, Soker S, Mukhopadhyay D. Neuropilin-1-mediated vascular permeability factor/vascular endothelial growth factor-dependent endothelial cell migration. J Biol Chem 2003;278:48848–60.
40. Takahashi F, Akutagawa S, Fukumoto H, et al. Osteopontin induces angiogenesis of murine neuroblastoma cells in mice. Int J Cancer 2002;98:707–12.
41. Senger DR, Ledbetter SR, Claffey KP, Papadopoulos-Sergiou A, Peruzzi CA, Detmar M. Stimulation of endothelial cell migration by vascular permeability factor/vascular endothelial growth factor through cooperative mechanisms involving the αvβ3 integrin, osteopontin, and thrombin. Am J Pathol 1996;149: 293–305.
42. Shijubo N, Uede T, Kon S, et al. Vascular endothelial growth factor and osteopontin in stage I lung adenocarcinoma. Am J Respir Crit Care Med 1999;160: 1269–73.
43. Shijubo N, Uede T, Kon S, Nagata M, Abe S. Vascular endothelial growth factor and osteopontin in tumor biology. Crit Rev Oncog 2000;11:135–46.
44. Giavazzi R, Nicoletti MI. Small molecules in anti-angiogenic therapy. Curr Opin Invest Drugs 2002;3: 482–91.
45. Kerbel RS, Viloria-Petit A, Klement G, Rak J. 'Accidental' anti-angiogenic drugs. anti-oncogene directed signal transduction inhibitors and conventional chemotherapeutic agents as examples. Eur J Cancer 2000;36:1248–57.
46. Jain S, Chakraborty G, Bulbule A, Kaur R, Kundu GC. Osteopontin: an emerging therapeutic target for anticancer therapy. Expert Opin Ther Targets 2007;11:81–90.